



Simulating submarine landslides combining the material point method with a spatially adaptive scheme to improve numerical accuracy

Lucas D. F. Lino¹, Tiago P. S. Lôbo¹

¹Laboratory of Scientific Computing and Visualization, Federal University of Alagoas
Av. Lourival Melo Mota, S/N, Tabuleiro do Martins, 57072-900, Maceió/AL, Brazil
lucaslino@lccv.ufal.br; tiago@lccv.ufal.br

Abstract. Particles, in the material point method (MPM), are the representation of the material domain, which moves through a background mesh. As deformation occurs, particles positions are updated accordingly and may generate regions with suboptimal particle density. In cases with excessive tractions, increased deformations can make distance between particles to be greater than the background mesh element size, causing fractures to occur in materials where no fracture law was applied. Moreover, this numerical fracture undermines computational accuracy and stability of the simulations. Therefore, a spatially adaptive method is a suitable alternative to prevent the formation of numerical fractures in problems with large deformations. Furthermore, spatial adaptivity, a technique that tunes the spatial discretization of the problem dynamically, has already been used to simulate engineering problems with large deformations and complex soil-structure interactions. However, such simulations are unstable depending on the material constitutive model and the computational cost is quite expensive. This study proposes a spatially adaptive algorithm based on the accumulated deformation of each particle. The algorithm divides each particle into four new ones that inherit the quantities of interest from old particles, maintaining the continuity of state variables. The algorithm showed to be efficient in problems with analytical solutions, such as the vibration of an elastic bar. In addition, as submarine landslides involve large deformations, numerical fractures are bound to happen and often imposes constraints to the scale of the mesh discretization. In this regard, our algorithm handled, successfully, submarine landslides simulations, introducing new particles to regions that presented a poor distribution of particles during the sliding process, enhancing the visual aspect and allowing a correct computation of state variables. Lastly, the spatial adaptivity scheme was coupled into the software E-Sub, a numerical analysis software developed by the Laboratory of Scientific Computing and Visualization (LCCV).

Keywords: GIMP, submarine landslides, spatial adaptivity, numerical fractures

1 Introduction

Oil and gas sub-sea structures can be located near submarine slopes and, consequently, might be exposed to geohazards, such as submarine landslides. The sliding process of the soil mass, which can be motivated by natural causes, such as earthquakes, or human interventions, poses a threat to sub-sea equipment structural integrity. In this regard, due to submarine landslides potential socioeconomic and environmental impacts, there has been increasing interest in their cause and effect.

When accumulated, unstable sediments might collapse when submitted to small perturbations. The resulting landslide and associated turbidity currents are responsible for depositing immense volume of debris into deep water. These deposits might be located thousands of kilometers away from the original site. Moreover, the submarine landslide geologic scale and time magnitude of its occurrence, most of which are dated from the glacial period [1], turns monitoring and studying these events into a difficult task. Hence, alternatives to analyze these events are required and, in this work, we turn our attention to numerical simulations.

Using an appropriate numerical method that can handle both large displacements and deformations is essential to study submarine landslides. The material point method (MPM) is a Lagrangian method created to solve problems involving large deformations and history-dependent constitutive equations, which are crucial aspects when simulating submarine landslides. The MPM can be seen as an extension of the finite element method (FEM)

in which, to avoid mesh distortion, the domain is further discretized into Lagrangian particles (material points that carry all material information) that move through a background finite element mesh whereby the equations of motion are solved. As particles move through the background mesh, their spatial configuration can change completely. In some cases, particles belonging to the same body can be separated by distances greater than a background mesh element size and the number of particles in an element can be greatly reduced. Such situations introduce numerical errors and might create fractures even though no fracture law is defined [2].

In order to maintain continuity of the body and circumvent numerical fractures, one can recur to spatially adaptive schemes, such as particle resampling techniques and dynamically mesh refinement. In engineering problems, spatial adaptivity techniques have been used in simulations such as: crack propagation and mudmat impact by submarine landslides [3, 4]. However, these techniques are computationally expensive and might not work on materials with complex history-dependent parameters.

In this study, we present a spatially adaptive algorithm, enhancing discretization and dynamically allocating more particles according to their deformation, that works on materials with complicated history-dependent parameters. Additionally, we focused on demonstrating that the adaptive procedure does not modify the initial problem solution and conserve energy. In order to ensure energy conservation and the mechanical state of the system, we directly assign old state variables to the resampled particles. The developed algorithm was implemented in C++ and integrated into an in-house developed MPM program.

2 Material point method

In the material point method (MPM), a continuum body is represented as a set of Lagrangian particles, which carry all information with them (e.g., mass, density, energy, stress, strain and other constitutive model state variables), and move through a finite element background mesh in which the equations of motion are solved. From here on out the subscript i will denote variables evaluated at the node i , the subscript p indicates that the quantity is evaluated at the position of particle p and the superscript k denotes evaluation at the time $t = k \cdot \Delta t$, in which Δt is the time step. Moreover, the update stress last (USL) integration scheme is used in this work.

The solution procedure of a dynamical problem, in MPM, involves solving the same four stages every time step. The first stage in a time step, Fig. 1a, is the mapping of quantities (e.g., mass and momentum) from material points to the background mesh nodes using $f(\mathbf{x}_i) = \sum_p f(\mathbf{x}_p)N_i(\mathbf{x}_p)$, in which f is the quantity being mapped, $N_i(\mathbf{x})$ is the shape function of node i and \mathbf{x} is the position [3]. The second stage, depicted in Fig. 1b, is the calculation of nodal forces using $\mathbf{M}_i^k \mathbf{a}_i^k = \mathbf{f}_i^{int,k} + \mathbf{f}_i^{ext,k}$, in which \mathbf{M} is the lumped mass matrix, \mathbf{a} is the acceleration, \mathbf{f}^{int} is the internal force and \mathbf{f}^{ext} is the body force. In the third stage, nodal forces are mapped back to the particles, Fig. 1c, leaving the background mesh nodes positions unchanged (here lies the reason why the MPM avoids mesh distortion despite using a finite element mesh). In the last stage, shown in Fig. 1d, positions, velocities and the state of the particles are updated, in which the deformed background mesh can be discarded, if necessary, to use a new one in the next time step.

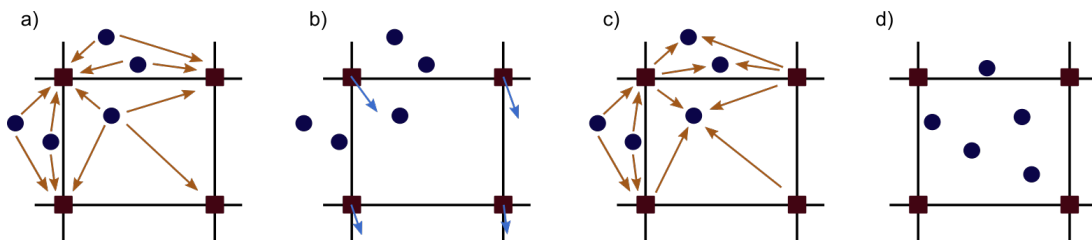


Figure 1. Scheme of the solution procedure of MPM for a single time step. Orange arrows indicate quantities of particles mapped to the spatial nodes and blue arrows indicate dummy nodal velocity values.

Traditional MPM suffers from some inconsistencies stemming from a poor discretization scheme (using Dirac's delta to spatially represent particles). In this work, we use the generalized interpolation material point (GIMP) [5] to avoid these inconsistencies. In GIMP, particles are defined by a characteristic function $\chi_p(\mathbf{x})$ and, thus, they always occupy a non-zero volume in space, solving these problems from the original MPM implementation. As a consequence of using characteristic functions to represent particles, the only change on traditional MPM equations is the replacement of shape functions and its gradient by the integral of themselves times the particle characteristic function over a particle domain.

Constitutive modelling of submarine landslides requires history-dependent constitutive properties, which can be addressed by the MPM. During the sliding process, as the soil mass is remoulded and water gets progressively more entrained, shear strength is degraded, reducing its magnitude [6]. The Herschel-Bulkley rheological

model, which is an extension of the elastoplastic von Mises model, accounts for these effects (rate-dependent shear strength, with the undrained shear strength being modified along the sliding process) and is commonly used to describe the sliding material. In this study, we use the von Mises constitutive model, with a constant undrained shear strength, to assume rate-independent flow.

3 The spatially adaptive algorithm

As submarine landslides involve large deformations and displacements, numerical fractures are bound to happen. Moreover, numerical fractures not only worsen the appearance of the simulation, as shown in Fig. 4a, but also lead to incorrect computation of state variables as integration error is highly increased. In order to understand why a numerical fracture leads to numerical errors, one can interpret the material points as the number of points of a numerical integral. As regions have less particles, before a fracture is even developed, the quantitative response is already compromised due to its coarse representation. In this regard, we developed a spatially adaptive algorithm that detects and splits particles possessing large deformations into newer ones, increasing particle density and avoiding numerical fractures.

As discussed in section 2, we update all material point variables during the last stage of a single time step (Fig. 1d). At the end of this stage, after the update of a particle, we introduced a rule that decides if a particle will be split, based on its current and initial deformation fields. A particle is subdivided if their current length, $L_{current}$, is much bigger than its initial length, $L_{creation}$ (length with which it was created):

$$L_{current} > \beta \cdot L_{creation} \therefore (1 + \epsilon_{current}) > \beta \cdot (1 + \epsilon_{creation}); \quad (1)$$

in which β is a user-defined limiting parameter. The limiting parameter tells us how much a particle can deform without being split, and needs to be adjusted depending on the problem. We observed that submarine landslides simulations responses are good within a range of β values from 1.4 to 1.7 (i.e., particles are split if their current deformation becomes 30% to 70% higher than their initial deformation). This way, if given very small values, all particles would be divided at every time step, which is completely impracticable to simulate, and if given very high β values, no particle would be divided throughout the whole simulation.

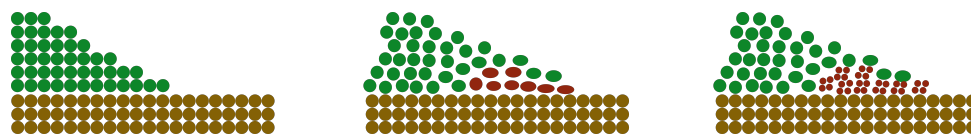


Figure 2. Representation of the division of particles during a submarine landslide. Brown particles represent the fixed seabed and the soil mass is represented by green or red particles. As the sliding process start, particles with initially acceptable strain values (green particles), start to deform. As deformation of particles exceeds the predefined limit (red particles), division is performed. Particles now become four new ones, receiving the current deformation field; positions are adjusted accordingly and conservation of quantities is maintained.

During the evaluation of the deformation of a particle, if condition of eq. (1) is met, the particle is subdivided into four new ones with the same stress and strain fields of the original particle, as shown in Fig. 2. The assumption that the stress and strain are constant in the region occupied by a material point is inherited from the initial assumptions of the generalized material point method, as stated by Bardenhagen and Kober [5] in equation 6 of the original GIMP paper.

The four new particles will directly receive state variables such as velocity, acceleration and internal variables of the constitutive model. Mass, volume, weight and initial length are divided equally between the new particles. As deformation and kinetic energy are functions of the volume and mass of a particle, respectively, conservation of mechanical energy is guaranteed when using the proposed split scheme. Furthermore, the new initial positions (x_{new} and y_{new}) will take into account the current length and positions of the old particle ($L_{current}$, x_{old} and y_{old}) and a correction based on the axial accumulated strain of the old particle (ϵ_{xx} and ϵ_{yy}):

$$\begin{aligned} x_{new} &= x_{old} \pm (1 + \epsilon_{xx}) \cdot (L_{current}/4); \\ y_{new} &= y_{old} \pm (1 + \epsilon_{yy}) \cdot (L_{current}/4). \end{aligned} \quad (2)$$

4 Results

As a first demonstration of the efficiency of our technique, we will show that the solution of the axial vibration of a continuum bar [7] remains unchanged when we apply our spatially adaptive scheme. We consider a linear elastic bar, with Elastic modulus $E = 10kPa$ and zero Poisson's ratio, fixed at the left side ($x = 0$), with length

L and density $\rho = 1000kg/m^3$, Fig. 3a. The generic solution is an infinite series [7] and can be simplified by considering only a single k -mode solution. Considering as initial conditions $u(x, 0) = 0$ and $\dot{u}(x, 0) = v(x, 0) = v_0 \sin(\beta_k x)$, we have $u(x, t) = \frac{v_0}{\omega_k} \sin(\omega_k t) \cos(\beta_k x)$ and $v(x, t) = v_0 \cos(\omega_k t) \sin(\beta_k x)$, in which $\omega_k = (2k - 1)\pi c/2L$ is the natural frequency of mode k , $c = \sqrt{E/\rho}$ is the wave velocity, $\beta_k = (2k - 1)\pi/2L$, v and u are the velocity and the displacement of the bar, respectively. Specifically, we analyzed the $k = 1$ mode, with time step $\Delta t = 0.1\sqrt{E/\rho}$, 4 particles per element, a regular Q4 background mesh with element size of $0.50m$ and $v_0 = 0.1m/s$.

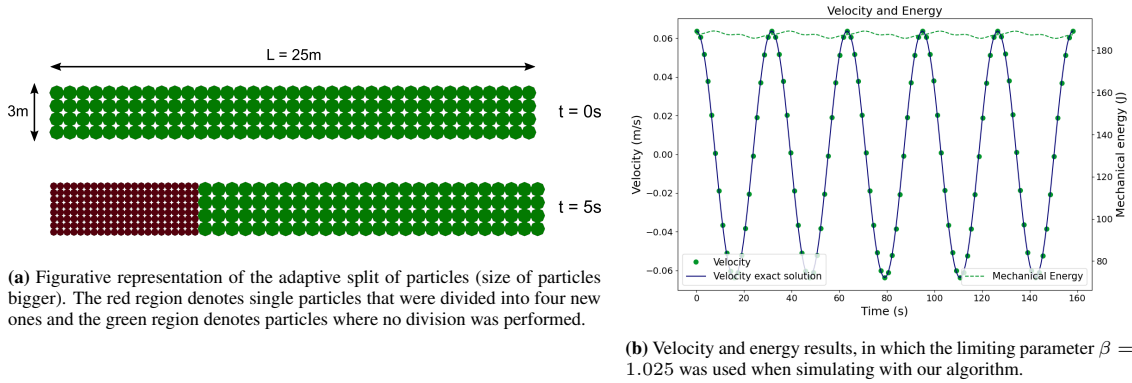
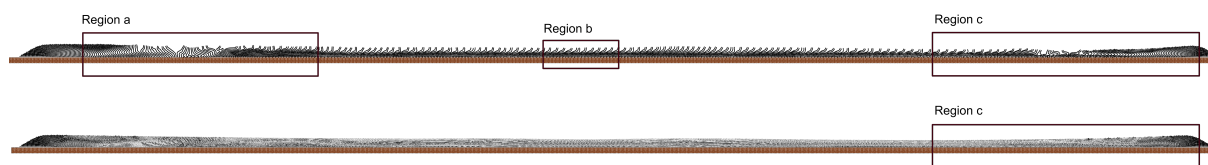


Figure 3. Results of the axial vibration of a continuum bar.

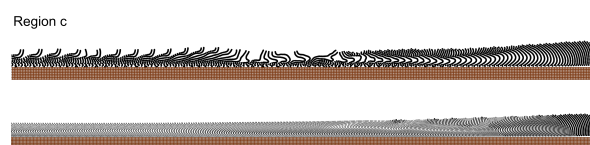
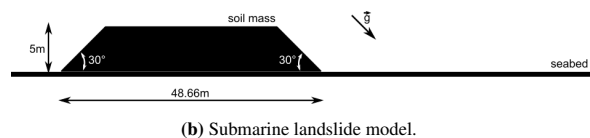
In the results depicted in Fig. 3a and Fig. 3b we considered a limiting parameter of $\beta = 1.025$. This means that if a particle length gets 2.5% greater than its initial length, it will be replaced by four new ones. It should be mentioned that this problem does not need a spatially adaptive treatment for the conditions considered. Nevertheless, its use provides a good benchmark for the proposed adaptive procedure. The analytical solution predicts an increased deformation, mostly on the left side of the bar, due to the initial conditions applied. Consequently, it is expected that particles located on this region will subdivide based on β (as shown in Fig. 3a). The numerical solution shows good agreement with the analytical one, even after particles subdivisions, as shown in Fig. 3b. Finally, energy conservation is also observed, as our technique do not affected the computation of the state variables.

With the consistency of the proposed technique ensured, one might want to put it to test in a more complex scenario. We chose a submarine landslide case solved previously by Dong [6]. In this example, the mobilized mass of a submarine landslide is simulated under undrained conditions, with an undrained shear strength of $su_0 = 2.5kPa$. Its initial geometry is assumed to be trapezoidal, with $48.66m$ and $5m$ of length and height, respectively (Fig. 4b). The maximum mobilized shear stress in the interface between the soil mass and the seabed is assumed to be $\tau = 1kPa$ and a Coulomb friction coefficient of $\mu_m = 10$ is also considered. Additionally, to better represent the contact between the seabed and the soil mass, we rotated the gravity an amount of 5° and kept the seabed aligned with the x axis. This allows a better representation of surface normals of the seabed in the background mesh. The soil mass is assumed to be elastic with a perfectly plastic von Mises yield criterion ($E = 250kPa$, $\nu = 0.49$ - to simulate constant volume, submerged density $\rho = 600kg/m^3$ and yield stress $\sigma_y = \sqrt{3} \cdot su_0$). The MPM simulation is run with 4 particles per element, an element size of $0.20m$ and a time step of $\Delta t = 0.2\sqrt{E(1-\nu)/((1+\nu)(1-2\nu)\rho)}$.

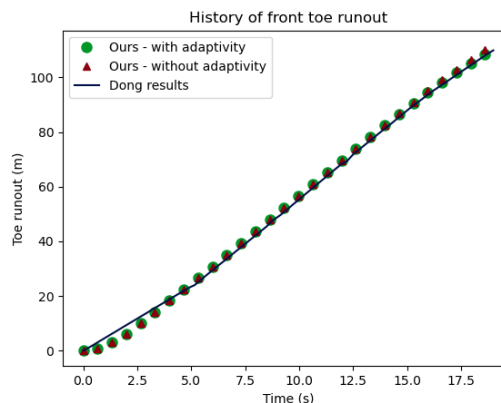
We used a limiting parameter of $\beta = 1.40$ to better capture the evolution of the strain field during the sliding process, inducing particles to be replaced in regions with large deformations and susceptible to numerical fractures. We observed that the final runout distance simulating with and without our adaptive scheme is similar to Dong results, Fig. 4d. Even so, both Dong and our simulation, without spatial adaptivity, present regions with scarce particle distribution and numerical fractures, inadequate to accurately capture the response of the sliding process, producing unreliable results for the stress and strain fields (Fig. 4a). Numerical fractures are developed during the sliding process due to the physical behavior of such phenomenons. The unstable backside of the initially trapezoidal soil mass collapses and the front part slides to the right due to its self-weight force, elongating and increasing the contact area with the seabed. Thus, friction force is increased, leading particles to endure substantial deformations. During this process, particles are separated due to these high traction deformations, generating numerical fractures, which was observed in both Dong and our simulation (without spatial adaptivity). When using our algorithm, particles are split according to the increase of their deformation, populating regions previously presenting poor particle distribution, Fig. 4c, thus remedying numerical integration inconsistencies and producing a more reliable result to the simulation of submarine landslides.



(a) Submarine landslide complete visualization of the sliding process. Here, we highlight regions presenting a poor particle distribution in the simulation without the adaptive algorithm.



(c) Comparison of region c with a poor particle distribution (without our algorithm) and a good particle distribution (with the adaptive scheme) depicted from the submarine landslide simulation. When used our adaptive scheme, the limiting parameter was taken as $\beta = 1.4$.



(d) Runout history of the front toe of the sliding mass (particle located to the most right during the sliding process).

Figure 4. Submarine landslide model and results.

5 Conclusions

This study presented the application of a spatially adaptive algorithm into the MPM and applied it on submarine landslides. The proposed algorithm preserves energy while increasing the quality of the solution. Furthermore, we showed that simulations of submarine landslides with the MPM are prone to present numerical fractures and undersampled regions, degrading numerical accuracy. Our methodology eliminates numerical fractures from submarine landslides simulations, increasing solution quality.

Acknowledgements. This study was supported by the Laboratory of Scientific Computing and Visualization (LCCV). The first author would like to acknowledge the advises and cooperation of the LCCV researchers of MPM research group throughout the development of this work.

Authorship statement. The authors hereby confirm that they are the sole liable persons responsible for the authorship of this work, and that all material that has been herein included as part of the present paper is either the property (and authorship) of the authors, or has the permission of the owners to be included here.

References

- [1] E. O. Nisbet and D. J. Piper. Giant submarine landslides. *Nature*, vol. 392, n. 6674, pp. 329–330, 1998.
- [2] X. Zhang, K. Y. Sze, and S. Ma. An explicit material point finite element method for hyper-velocity impact. *International Journal for Numerical Methods in Engineering*, vol. 66, n. 4, pp. 689–706, 2006.
- [3] H. Tan and J. A. Nairn. Hierarchical, adaptive, material point method for dynamic energy release rate calculations. *Computer Methods in Applied Mechanics and Engineering*, vol. 191, n. 19-20, pp. 2123–2137, 2002.
- [4] Y. Dong. Reseeding of particles in the material point method for soil–structure interactions. *Computers and Geotechnics*, vol. 127, 2020.
- [5] S. G. Bardenhagen and E. M. Kober. The generalized interpolation material point method. *CMES - Computer Modeling in Engineering and Sciences*, vol. 5, n. 6, pp. 477–495, 2004.
- [6] Y. Dong. *Runout of submarine landslides and their impact on subsea infrastructure using material point method*. PhD thesis, The University of Western Australia, 2017.
- [7] S. G. Bardenhagen. Energy conservation error in the material point method for solid mechanics. *Journal of Computational Physics*, vol. 180, n. 1, pp. 383–403, 2002.